J. Biochem. 2012;152(3):259–268 doi:10.1093/jb/mvs058

JB THE JOURNAL OF BIOCHEMISTRY

Critical roles of the mitochondrial complex II in oocyst formation of rodent malaria parasite *Plasmodium berghei*

Received May 1, 2012; accepted May 16, 2012; published online May 23, 2012

Akina Hino[1,*], Makoto Hirai[2,3,*†], Takeshi Q. Tanaka[1,‡], Yoh-ichi Watanabe[1], Hiroyuki Matsuoka[3] and Kiyoshi Kita[1,§]

[1]Department of Biomedical Chemistry, Graduate School of Medicine, The University of Tokyo, 7-3-1 Hongo, Bunkyo-ku, Tokyo 113-0033, Japan; [2]Department of Parasitology, Graduate School of Medicine, Gunma University, 3-39-22 Maebashi City, Gunma 371-8511, Japan and [3]Division of Medical Zoology, Department of Infection and Immunity, School of Medicine, Jichi Medical University, Shimotsuke City, Tochigi 329-0498, Japan

*These authors contributed equally to this study.

†Makoto Hirai, Department of Parasitology, Graduate School of Medicine, Gunma University, 3-39-22 Maebashi City, Gunma 371-8511, Japan. Tel: +81-27-220-8023, Fax: +81-27-220-8025, email: makotohirai@gunma-u.ac.jp

‡Present address: Laboratory of Malaria and Vector Research, National Institute of Allergy and Infectious Diseases, National Institutes of Health, Rockville, MD 20892, USA.

§Kiyoshi Kita, Department of Biomedical Chemistry, Graduate School of Medicine, The University of Tokyo, 7-3-1 Hongo, Bunkyo-ku, Tokyo 113-0033, Japan. Tel: +81-3-5841-3528, Fax: +81-3-5841-3444, email: kitak@m.u-tokyo.ac.jp

It is generally accepted that the mitochondria play central roles in energy production of most eukaryotes. In contrast, it has been thought that *Plasmodium* spp., the causative agent of malaria, rely mainly on cytosolic glycolysis but not mitochondrial oxidative phosphorylation for energy production during blood stages. However, *Plasmodium* spp. possesses all genes necessary for the tricarboxylic acid (TCA) cycle and most of the genes for electron transport chain (ETC) enzymes. Therefore, it remains elusive whether oxidative phosphorylation is essential for the parasite survival. To elucidate the role of TCA metabolism and ETC in malaria parasites, we deleted the gene for flavoprotein (Fp) subunit, *Pbsdha*, one of four components of complex II, a catalytic subunit for succinate dehydrogenase activity. The Pbsdha(-) parasite grew normally at blood stages in mouse. In contrast, ookinete formation of Pbsdha(-) parasites in the mosquito stage was severely impaired. Finally, Pbsdha(-) ookinetes failed in oocyst formation, leading to complete malaria transmission blockade. These results suggest that malaria parasite may switch the energy metabolism from glycolysis to oxidative phosphorylation to adapt to the insect vector where glucose is not readily available for ATP production.

Keywords: complex II/malaria parasite/mitochondria/*Plasmodium berghei*.

Abbreviations: AP, alkaline phosphatase; BCIP, 5-bromo-4-chloro-3'-indolylphosphatase *p*-toluidine salt; Cyt *b*, cytochrome *b*; Cyt *c*, cytchrome *c*; DHOD, dihydroorotate dehydrogenase; ETC, electron transport chain; FAD, flavin adenine dinucleotide; FBS, fetal bovine serum; Fp, flavoprotein; FRD, fumarate reductase; HRP, horse radish peroxidase; Ip, iron–sulphur cluster protein; MQO, malate–quinone oxidoreductase; MV, methylviologen; NAD, nicotineamide adenine dinucleotide; NBT, nitroblue tetrazolium chloride; NDH2, type2 NADH–ubiquinone oxidoreductase; Q, quinine; QFR, quinol–fumarate reductase; SDH, succinate dehydrogenase; SQR, succinate–ubiquinone reductase; TBS, tris buffered saline; TCA, tricarboxylic acid.

Malaria is one of the most serious diseases in the world. It causes one million infant deaths and over 500 million clinical cases annually, of which 85% is in sub-Saharan Africa (*1*). The drugs such as pyrimethamine/sulphadoxine, chloroquine or artesunate are the common treatment against malaria, but there is the emergence and spread of drug-resistant malaria parasites throughout the world (*2*), resulting in an urgent need for new drug.

The mitochondrion of *Plasmodium* species is obvious target of antimalarial drugs, but the physiological importance of this organelle is poorly understood. In other eukaryotes, pyruvate dehydrogenase is localized in mitochondria where it links the glycolysis metabolic pathway to TCA cycle, while it is localized in the apicoplast in *P. falciparum* (*3*). Therefore, it has been unclear until recently how glycolysis metabolism is connected to the tricarboxylic acid (TCA) cycle. Blood-stage *P. falciparum* have only a single mitochondrion without crista (*4*). Such morphologically immature mitochondrion suggests that, unlike other eukaryotes, the blood stage *P. falciparum* relies mainly on cytoplasmic glycolysis for their energy metabolism but not on mitochondrial oxidative phosphorylation (*5*, *6*). Beside, recent omics-based studies showed that *P. falciparum* expressed all TCA cycle enzyme genes and most ones for the electron transport chain (ETC), and that *P. falciparum* produced the intermediates of the TCA cycle (*7*). Moreover, the genes for TCA cycle are upregulated at mosquito stages (*8*). The gametocytes, precursor cells of gametes possess mitochondria with cristae (*9*). These data suggest that mitochondrial energy metabolism may have more crucial roles in insect stages than blood stages,

which have not been intensively investigated until recently.

The mitochondrial complex II (succinate–ubiquinone reductase: SQR) oxidizes succinate to produce fumarate as a TCA cycle member enzyme. In the anaerobic electron transfer system, complex II carries out fumarate reduction using quinol as an electron donor (quinol–fumarate reductase; QFR), which is the reverse reaction of SQR. Complex II consists of four subunits, flavoprotein (Fp), iron–sulphur cluster protein (Ip) and two small membrane anchor subunits, cytochrome *b* large (CybL) and small (CybS) subunits. The Fp with molecular mass of 70 kDa has a flavin adenine dinucleotide (FAD) covalently bound to a highly conserved histidine (His) residue. Fp and Ip form catalytic portion of the complex and this portion acts as a succinate dehydrogenase (SDH), catalyzing the oxidation of succinate by water-soluble electron acceptors such as phenazine methosulphate in SQR, while it acts as a fumarate reductase (FRD), catalyzing electron transfer from water-soluble electron donors such as reduced methylviologen (MV) to fumarate in QFR. FAD in the Fp receives the reducing equivalents from succinate and then transfers it to quinone by SQR activity where the two small membrane anchor subunits are indispensable (*10*). Thus, complex II functions as a link between the TCA cycle and the ETC, directly. While complex II has such critical roles in energy metabolisms, and Fp and Ip subunits genes are substantially conserved in various organisms (*3*, *11*), two small membrane anchor subunit genes are diverse and had not been detected in the genomes of *Plasmodium* spp., suggesting that plasmodial complex II is nonfunctional. However, recently our intensive database mining has identified putative plasmodial anchor subunit genes (*12*). Moreover, biochemical studies revealed that SQR activity of complex II was detected in the mitochondrial fraction of *P. yoelii* and *P. falciparum*, and the activity was inhibited by the ubiquinone-binding site inhibitor, atopenin A5 (*13–15*).

In this work, we took genetic approach to understand the physiological role of the parasite complex II using *P. berghei* as a model because the whole parasite life cycle can be monitored using mosquito and mouse as hosts. We generated transgenic *P. berghei* (Pbsdha(-)) in which the Fp subunit gene (*Pbsdha*) of complex II was deleted to inactivate complex II activities. By infecting mice and mosquitoes with the Pbsdha(-) parasites, we followed phenotype of the Pbsdha(-) parasite during the whole life cycle and found that complex II is essential for oocyst formation in the mosquito.

Materials and Methods

Maintenance of mosquitoes and parasites

Anopheles stephensi (SDA 500 strain) and *P. berghei* (ANKA clone 2.34) were maintained as described previously (*16*). *P. berghei*-infected mosquitoes were fed on naïve mice (Balb/c), and the resulting infected mice were referred to as passage 0 (P0). The P0 blood was injected intraperitoneally to the naïve mice and the passage one (P1) mice were used in the experiments. The experiments using animals and recombinant DNA were performed under the guidelines of the committee in Jichi University, and assigned permission no. is 08-14.

Generation of Pbsdha::AGFP parasites

The two fragments covering the 5'UTR and the first 60 amino acids (−3229 to +180 bp), and 3′ UTR (1025 bp) of *Pbsdha* gene (PBANKA_051820) were amplified with primer pairs 5′UTRB4F/5′UTRB1R and 3′UTRB2F/3′UTRB3R, and *P. berghei* genomic DNA as template. The *Azami Green Fluorescent Protein* gene (*AGFP*) was amplified with the primers AzamiB1F/AzamiB2R. Each PCR fragment was cloned into *pDONRP4-P1R*, *P1-P2R* and *P2-P3R* vectors by BP clonase reaction (Invitrogen) to generate entry vectors (*5UTR*/*P4P1*, *AGFP*/*P1P2* and *3UTR*/*P2P3*). An R4-R3 fragment (Invitrogen) was inserted into *HindIII* site of *pBS-DHFR* vector (*17*) to generate an acceptor plasmid (*R4R3*/*pBS-DHFR*). The inserts of entry vectors were transferred to the acceptor plasmid by LR reaction using the Multisite Gateway Three-Fragment Vector Construction Kit (Invitrogen). In the final plasmid (*Pbsdha::AGFP*), 5' UTR and the first 60 amino acids of *Pbsdha* were fused to the *AGFP* gene. Thus, the expression of the *AGFP* reporter gene is under the control of the *Pbsdha* gene promoter. For parasite transfection, the plasmid was digested by *BstXI*, and the linearized plasmid was integrated into the parasite genome by single crossover homologous recombination. The parasite transfection and subsequent cloning were performed as described elsewhere (*18*). Correct integration events in Pbsdha::AGFP parasites clones were confirmed by Southern blot as described later in the text. The genomic DNA (10 μg) of Wild Type (WT) and Pbsdha::AGFP parasites was digested with *PacI* and *HpaI*, separated by 0.8% (w/v) agarose gel and transferred to the Hybond-N+ membrane (GE healthcare). PCR fragment (F1-HindIII/R1-HindIII) was labeled with AlkPhos Direct Labeling Reagent Kit (GE Healthcare) and used as probe for hybridization. The hybridization and washing were performed by following the manufacturer's protocol.

The expression of the AGFP gene at each developmental stage in Pbsdha::AGFP parasites was investigated as follows. To prepare the parasites at blood stages, the mouse blood (1 ml) infected with Pbsdha::AGFP parasites was collected, mixed with 120 ml RPMI1640 containing 25% fetal bovine serum (FBS) and cultured at 37°C for 16 hr by the candle-jar method (*19*). The parasites synchronized to schizonts were partially purified by Nycoprep 1.077 (*18*) and injected intravenously into mice tail veins. At 4 hr and 33 hr after injection, the parasites were synchronized to ring and trophozoite stages, respectively. A drop of tail blood was collected at these time points, and the AGFP signal in rings, trophozoites, and *in vitro* cultured schizonts was observed. For the analysis of AGFP expression in mosquito-stage parasites, the ookinetes were prepared *in vitro* as described in 'Examination of Pbsdha(-) parasite development'. The mosquitoes were fed on mice carrying Pbsdha::AGFP parasites and dissected on day 14 and 16 after the feeding. The AGFP signal in the oocysts (on midguts) and sporozoites (in salivary glands) as well as *in vitro*-cultured ookinetes was observed. The parasite was stained with 10 nM of MitoTracker Orange CMTM Ros (Molecular Probes) and DAPI (4′,6-diamino-2-phenylindole) (Dako) to label mitochondria and nuclei, respectively. The fluorescent signal of MitoTracker, DAPI and AGFP was detected at 540 nm, 452 nm and 520 nm, respectively.

Targeted disruption of the Pbsdha gene

Two regions of the *Pbsdha* gene were amplified by PCR using primer pairs F1-HindIII/R1-HindIII and F2-EcoRI/R2-BamHI, and *P. berghei* genomic DNA as template. The PCR fragments were digested with respective restriction enzymes and cloned to *pBS-DHFR* to give a targeting plasmid, *pPbsdha(-)*. The *pPbsdha(-)* plasmid was digested with *ClaI* and *BamHI*, and the plasmid was introduced in *P. berghei* by electroporation. The correct recombination event of the clones was confirmed by diagnostic PCR using two primer sets, K1 (K1-F and R) and K2 (K2-F and R). Correct integration was also checked by Southern blot analysis as described earlier in the text. The genomic DNA of WT and Pbsdha(-) parasites was digested with *PacI*, and a PCR fragment (F1-HindIII/R1-HindIII) was used as probe. The contamination of WT parasites in Pbsdha(-) parasite clone was checked by PCR with primer set W (W-F and R). Two clones from two independent transfection experiments were isolated and analyzed further. All primer sequences are described in supplementary information.

Western blot analysis of mitochondrial fraction

The mitochondrial fractions were prepared from mouse leucocytes, *in vitro* cultured *P. falciparum*, and WT and Pbsdha(-) of *P. berghei* by N_2 cavitation methods (*13*, *14*). The mitochondrial fractions of mouse liver (10 μg/lane), WT and Pbsdha(-) of *P. berghei* (20 μg/lane) and *P. falciparum* (10 μg/lane) were loaded onto 10% SDS polyacrylamide gel electrophoresis and transferred to a nitrocellulose membrane (Whatman). The membrane was blocked with SuperBlock (Pierce) and washed with TBS-T (150 mM NaCl, 0.05% (v/v) Tween 20, 10 mM Tris-HCl; pH 7.5). To detect the Fp subunit, the membrane was hybridized with antiserum against the *P. falciparum* Fp peptide (*20*) as primary antibody (1/1,000 dilution) and alkaline phosphatase (AP) conjugated anti-rabbit IgG antiserum as secondary antibody (1/10,000 dilution). The AP enzyme activity on the membrane was visualized by a chromogenic method using NBT and BCIP. To confirm the equal loading of the samples on the gel, *P. berghei* heat shock protein 70 (HSP70) was used as internal control. The same membrane used in Fp detection was rehybridized with anti-HSP70 antiserum as primary antibody (1/100 dilution) and horse radish peroxidase (HRP) conjugated anti-mouse IgG antiserum as secondary antibody (1/10,000 dilution). HRP enzyme activity was detected as chemiluminescent signal by the Immobilon Western Chemiluminescent HRP Substrate (Millipore).

Measurement of SQR activity in mitochondrial fraction

The SQR enzyme activity assay was performed at 25°C with a V-660 spectrophotometer (JASCO, Tokyo, Japan). The enzyme activity of SQR was determined as quinone-mediated succinate: 2,4-dichlorophenolindophonol (DCIP) reductase in 30 mM Tris-HCl (pH 8.0) containing 10 mM potassium succinate, 100 μM ubiquinone-2 and 45 μM DCIP ($\varepsilon^{600nm} = 21\,mM^{-1}cm^{-1}$) in the presence of 2 mM KCN and 0.1 μM Atpenin A5 (Alexis Biochemicals). Atpenin A5 was proven to be a novel inhibitor specific to mouse leukocytes but not parasitic SQR activity at this concentration in our previous study (*13*).

Examination of Pbsdha(-) parasite development

To assess the growth rate of the parasites in mice, the red blood cells (RBC) (10^4) infected with either WT or Pbsdha(-) parasites were intravenously injected into tail vein of each of the four naïve mice. Subsequently, the tail blood was taken every 24 hr and the number of infected RBCs was counted. To investigate the male gametogenesis, the infected blood (10 μl) was added to 1 ml of fertilization medium (10 % (v/v) FBS in RPMI1640 (pH 8.2)) at 21°C. The sample (10 μl) was taken at 15 min and the number of exflagellating male gametes was counted. The rest of the sample was further incubated for 16 hr and the number of ookinetes was counted. The fertilization rate was calculated by the conversion rate of female gametocytes into ookinetes.

Infectivity of Pbsdha(-) parasite to mosquito and transmission to mouse

The tail blood of WT- and Pbsdha(-)-infected mice was taken and the number of exflagellating male gametes was counted. Only the mice whose blood contained over 2 exflagellating centers per 10^4 RBC were used for the mosquito feeding. Female mosquitoes (4–7 days old) were fed on the infected mice, and fully engorged mosquitoes were collected. Sixteen days after blood feeding, midguts and salivary glands were isolated. The number of oocysts in the midgut was counted and the presence of sporozoites in the salivary gland was examined to assess the infectivity of the parasites to mosquitoes. To investigate the transmission efficiency to mice, more than 20 mosquitoes carrying WT or Pbsdha(-) parasites were fed on naïve mice. The transmission of the parasites to mice was examined by checking mouse blood smears until 2 weeks after the mosquito feeding.

Results

Identification and expression analysis of Pbsdha

We found PBANKA_051820 being annotated as a putative Fp subunit gene of complex II in PlasmoDB, and hereafter it is referred to '*Pbsdha*'. It is known that amino acid sequences of Fp are highly conserved among various organisms. As such, the amino acid sequence of *P. berghei* FP (PbFp) shows high identity to those of other organisms including *P. falciparum* Fp, which we have reported previously (*11*). Especially, histidine in the FAD binding site in the catalytic domain is completely conserved in PbFp (Fig. 1).

To investigate *Pbsdha* gene expression during parasite life cycle, we generated Pbsdha::AGFP parasites as a reporter line, in which *AGFP* reporter gene expression is regulated by the endogenous *Pbsdha* gene promoter (Fig. 2A). It is reported that the first 60 amino acids of *P. falciparum* Fp (PfFp) contain a functional mitochondrial targeting signal (*21*) and the corresponding amino acid sequence of PbFp shows 75% identity to that of PfFp (*11*), suggesting the same function in the corresponding region of PbFp. To investigate the cellular localization and developmental expression of AGFP during the parasite life cycle, the first 60 amino acids of PbFp was fused to AGFP (Pbsdha::AGFP). The WT parasites were transfected with the *Pbsdha::AGFP* plasmid and the correct integration event in Pbsdha::AGFP parasite clone was confirmed by Southern blot (Fig. 2B). For the analysis of cellular localization of AGFP, the Pbsdha::AGFP parasites were stained with MitoTracker Orange to label the mitochondrion. As shown in Fig. 2C, AGFP signals colocalized with MitoTracker Orange signals, indicating that the N-terminal sequence of PbFp possesses a functional mitochondrial targeting signal. Next, we investigated the reporter gene expression at each developmental stage of parasites in red blood cell. AGFP signal was detected in trophozoite and schizont (Fig. 2D) but not in the ring form stage (data not shown). To investigate the AGFP expression in the parasites at mosquito stages, Pbsdha::AGFP parasites were fed to mosquitoes. As shown in Fig. 2E, the signal was detected in *in vitro*-cultured ookinetes, and oocysts and sporozoites in mosquitoes. These results indicate that *Pbsdha* was expressed in both blood stages and mosquito stages.

Disruption of the Pbsdha gene

Then, to study the *P. berghei* complex II functions, we generated Pbsdha(-) parasites by replacing the *Pbsdha* gene with *TgDHFR* (Fig. 3A). Two independent clones (KO-a and KO-b) were established by independent transfection experiments. The correct targeting event in each clone was confirmed by Southern blot analysis (Fig. 3B) and diagnostic PCR (Fig. 3C). Following the confirmation of *Pbsdha* gene disruption, we further checked the deletion of the PbFp protein and SQR enzyme activity in Pbsdha(-) parasites by Western blot and enzyme activity assay, respectively. For these experiments, we prepared the crude mitochondrial samples from WT, Pbsdha(-) parasites, *in vitro* cultured *P. falciparum*, and naïve mouse liver. To detect the Fp peptide by Western blot analysis, we used the anti-PfFp antiserum (*20*) because the amino acid sequence of PfFp shows high identity to those of PbFp (90.5 %) and mice Fp (63.3 %). It is thus anticipated that the antiserum may cross-react to both PbFp and mice Fp proteins. As shown in Fig. 3D, the antiserum reacted to the peptides with expected size of

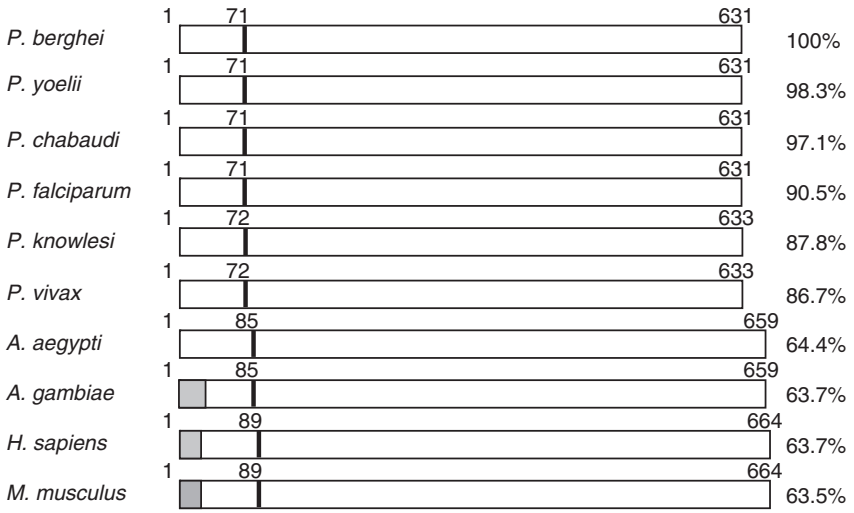

Fig. 1 Primary structure of Fp proteins from 10 species. The box indicates the full-length Fp protein. The mitochondrial sorting signal is colored in grey. The black line with number indicates the conserved His for FAD binding site. The total number of amino acid residues and the amino acid identity to PbFp are indicated on the right (%).

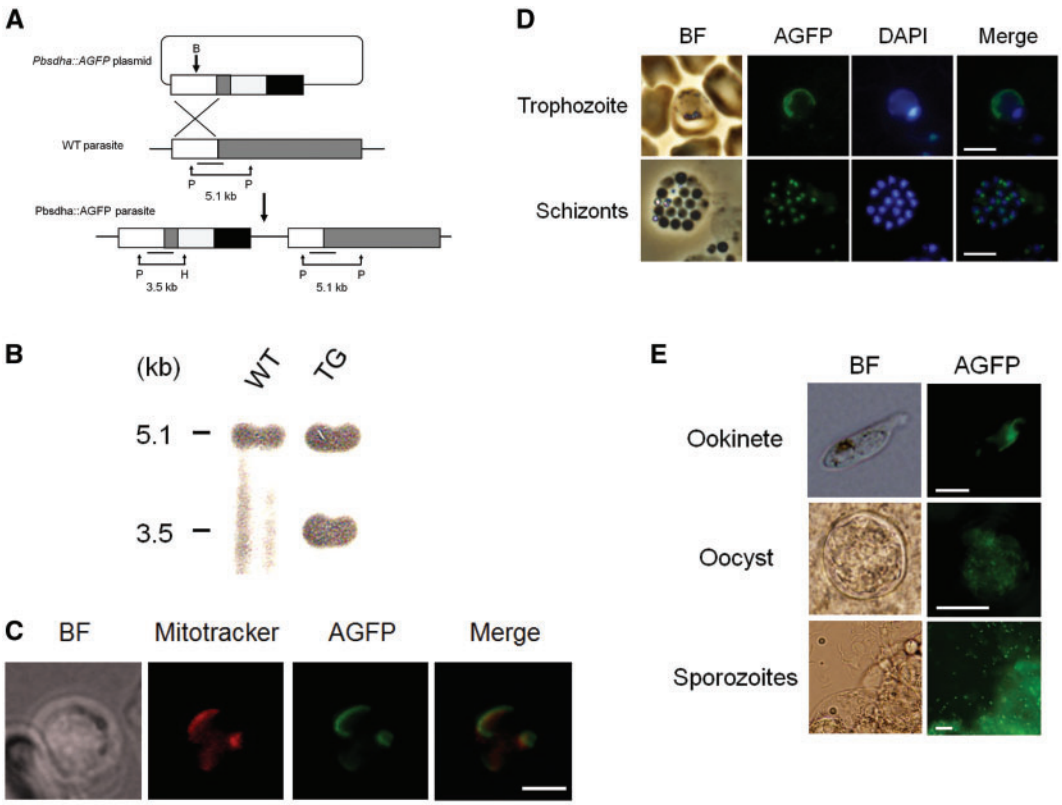

Fig. 2 Generation of the transgenic parasite line Pbsdha::AGFP. (A)Schematic representation of *AGFP* tagging of the *Pbsdha* locus using a plasmid that integrated through single crossover homologous recombination. In the *Pbsdha::AGFP* plasmid, the boxes indicate *Pbsdha* gene promoter (white), the first 60 amino acids of Pbsdha (dark gray), AGFP (light gray), 3′UTR of *Pbsdha* gene and *TgDHFR/ts* selectable marker cassette (black). In the *Pbsdha* gene locus (middle), the box with dark gray indicates full open reading frame of *Pbsdha*. B, H and P indicate *BstXI*, *HpaI* and *PacI* digestion sites, respectively. Bars represent the position of the probe used in Southern blot analysis. (B) Southern blot analysis of WT and Pbsdha::AGFP parasites. Hybridization of the probe with *PacI*- and *HpaI*-digested genomic DNA yielded a 5.1 kb for WT, and 3.5 kb and 5.1 kb for Pbsdha::AGFP parasites (TG). (C) Cellular localization of AGFP in Pbsdha::AGFP parasites. The mouse erythrocyte infected with Pbsdha::AGFP parasites was observed under bright field (BF). The signals of MitoTracker and AGFP in the same cell were detected through red (MitoTracker) and green filter (AGFP), respectively. Bar represents 5 μm. (D) Expression of *AGFP* gene in Pbsdha::AGFP parasites at blood stages. The AGFP signal was detected in the parasites synchronized at trophozoite (upper) and schizont stages (lower). Nuclei were stained with DAPI. Bars represent 5 μm. (E) Expression of the *AGFP* gene in Pbsdha::AGFP parasites at mosquito stages. The AGFP signal was detected in *in vitro* cultured-ookinetes, oocysts in the midguts and sporozoites in the salivary gland of mosquitoes. Bar represents 20 μm.

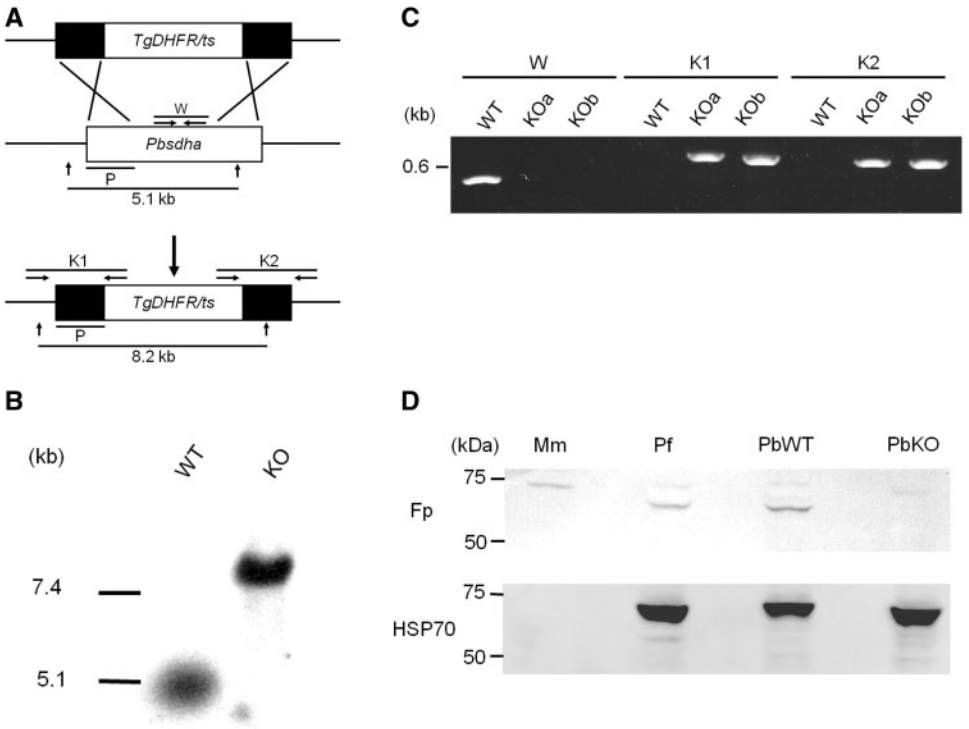

Fig. 3 Targeted disruption of the *Pbsdha* gene. (A) Schematic representation of the replacement strategy to generate Pbsdha(-) parasites. The WT *Pbsdha* gene locus is replaced with 5′ and 3′ UTRs of the *Pbsdha* gene and *TgDHFR*, a selectable marker. Vertical arrows indicate *PacI* site. P with bar indicates the probe position for Southern blot analysis. Arrows marked with W (WT specific) or K1/K2 (knockout specific) indicate the primer positions used in diagnostic PCR. (B) Southern blot genotyping confirmed integration. Hybridization of the probe with *PacI*-digested genomic DNA of WT and Pbsdha(-) parasites yielded a 5.1 kb and 8.2 kb band, respectively. (C) Confirmation of *Pbsdha* gene disruption by diagnostic PCR. Genomic DNA from WT, Pbsdha(-) clone A (KOa) and clone B (KOb) were used as templates. The positions of the PCR products in W and K1/K2 are depicted in Fig. 2A. (D) Detection of Fp peptides by Western blot analysis. The Fp peptides in mitochondrial fractions of *Mus musculus* (Mm), *P. falciparum*(Pf), *P. berghei* wild-type (PbWT) and Pbsdha(-) (PbKO) parasites were detected by anti-PfFp antiserum (upper panel). The anti-PbHSP70 antiserum was used to confirm equal loading of the protein samples in each lane (lower panel).

70.5 kDa (WT *P. berghei*) and 73.0 kDa (mice), as well as 70.7 kDa (*P. falciparum*). In contrast, no band was detected in Pbsdha(-) (PbKO) except for the high molecular weight band, which is speculated as contaminated mice Fp because the molecular weight of this faint band is similar to that of the band on Mm lane (Fig. 3D). The equal loading of each sample on the gel was confirmed by anti-PbHSP70 antiserum (lower panel in Fig. 3D). These results demonstrated that the PbFp protein was surely deleted from Pbsdha(-) parasites. Next, we investigated the SQR activity in Pbsdha(-) parasites by using the same samples used for Western blot analysis. While WT parasites showed an SQR activity of 4.38 ± 0.96 nmol/min/mg ($N = 3$), Pbsdha(-) did not show any detectable SQR activity (Table I). These results demonstrated that the PbFp protein and the SQR activity were completely eliminated from the Pbsdha(-) parasites.

Phenotypic analysis of Pbsdha(-) parasites

As the disruption of the *Pbsdha* gene was confirmed, phenotypic effect of the gene disruption on the parasite was analyzed. In erythrocytic stages, Pbsdha(-) parasites underwent normal development and differentiation into gametocytes, which were not significantly different from those of WT parasites ($P > 0.1$, Fig. 4 and Table II). Successful *Pbsdha* gene deletion indicates that the SQR enzyme is not essential for the survival of the parasite at asexual stages and sexual differentiation. The mitochondria of Pbsdha(-) parasites were stained with Mitotracker, indicating that disruption of *Pbsdha* did not affect the mitochondrial membrane potential (Fig. 5).

Next, we investigated the parasite development at mosquito stages. In *P. berghei*, an *in vitro* assay has been established that mimics the gametogenesis and fertilization taking place in the mosquito body (*22*). Using this system, we confirmed that the efficiency of male gametogenesis in Pbsdha(-) parasites was comparable with that of WT parasites (data not shown). However, Pbsdha(-) parasites showed severe defects in ookinete formation, the stage next to fertilization. The conversion rate of female gametes to ookinetes in Pbsdha(-) was significantly reduced to 17% of WT parasite ($P < 0.05$ ($N = 3$), Fig. 6A). We further investigated the infectivity of Pbsdha(-) parasites to mosquitoes and the subsequent transmission to mice. The mosquitoes were fed on mice carrying either Pbsdha(-) or WT parasites, and then these mosquitoes were dissected for the evaluation of parasite development at day 16 post-feeding. Interestingly, several independent experiments using two clones showed that no oocysts were detected in the midguts of mosquitoes fed on mice carrying Pbsdha(-) parasites, while oocysts

Table I. SQR activity of the mitochondrial fraction in WT and Pbsdha(-) parasites.

	Exp 1	Exp 2	Exp 3
WT	5.31	4.44	3.40
KO	0.00	0.00	0.00

The value represents SQR activity in each independent assay (nmol/min/mg protein)

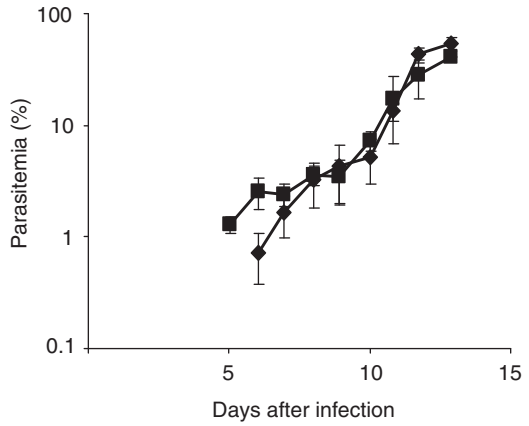

Fig. 4 The growth rate of intraerythrocytic stages of WT and Pbsdha(-) parasites. The parasitemia of WT and Pbsdha(-) parasites are indicated by closed square and diamond, respectively. Bar represents SD (N = 4).

Table II. The gametocytemia of WT and Pbsdha(-) parasites.

Parasites	Macrogametocytemia/ parasitemia	Microgametocytemia/ parasitemia
WT	6.5 ± 2.72	1.7 ± 0.45
KO	5.0 ± 1.11	1.5 ± 0.64

were detected in the mosquitoes fed on mice carrying WT parasites (Fig. 6B). Moreover, no transmission was observed in the mice challenged by the mosquitoes carrying Pbsdha(-) parasites, while WT parasites were transmitted to mice (Table III). Taken together, these results indicated that the development of Pbsdha(-) parasites was completely halted at the stage of oocyst formation.

Discussion

It is known that asexual stages parasites possess a single acristate mitochondria, while gametocytes, mosquito stages and preerythrocytic stage parasites possess five to six cristate mitochondria (*9*, *23*). This morphological maturation of mitochondria in the sexual stage parasites may correlate with the increased need of mitochondrial metabolism in the insect stage parasite development. Once malaria parasites are introduced to mosquitoes, they encounter to drastic environmental changes where the main sugar source is changed from glucose to torehalose, and they need to adapt to this (*24*). Our present work clearly shows that complex II has a critical role in parasite adaptation to the insect body. Namely, the parasite lacking complex II activity failed to form oocysts in mosquitoes, while the development of blood stage parasites in mice was not affected by *Pbsdha* gene disruption at all.

Developmental expression and targeting disruption of Pbsdha gene

By using Pbsdha::AGFP parasites as a reporter, we followed the AGFP expression during the whole parasite life cycle except for liver stage. Except for the ring stage, AGFP signals were detected in all developmental stages. It was reported that the size and morphology of mitochondria spectacularly changes during the life cycle and that the mitochondrial size is much smaller in the ring stage than in any other stage (*25*). Thus, the failure of signal detection in ring stage could be attributed to lower signal strength than the detection limit. According to gene expression data in PlasmoDB, the *P. falciparum* orthologous gene of *Pbsdha*, PF10_0334 is substantially expressed in all developmental stages including the ring form. Taken together, it can therefore be speculated that the *Pbsdha* gene is also expressed in all developmental stages.

In a global gene expression analysis, it was reported that several lines of *in vitro*-cultured *P. falciparum* showed very similar pattern in gene expression. In contrast, it was recently demonstrated that parasites derived directly from infected patients showed three distinct gene expression states (*26*). One of these states showed that the expression levels of *sdha* and other TCA cycle- or ETC-related genes are increased. Because such expression state has never been detected in *in vitro* studies and parasitic mitochondria are immature acristates, it had been considered that the blood-stage parasites mainly use cytosolic glycolysis and mitochondrial oxidative phosphorylation only marginally (Fig. 7). The discrepancy between the *in vivo* and *in vitro* studies above suggests that the parasites may use oxidative phosphorylation in *in vivo* in case that the patient would be hypoglycemic, which is reflected in the upregulation of the genes involved in oxidative phosphorylation. In the i*n vitro* system, on the other hand, glucose is continuously supplied in the medium and the environmental condition is artificially controlled, therefore the parasites may exclusively undergo glycolysis and the enzymes of oxidative phosphorylation may be marginally expressed. Thus, it is important to undertake experiments using both *in vitro* and *in vivo* systems in order to understand how parasites respond to various environmental stimuli. In this sense, the rodent malaria model could be an ideal tool to investigate the changes in parasite metabolism *in vivo*.

Complex II is essential for the parasite survival at mosquito stages

We successfully generated Pbsdha(-) parasites, confirmed by Southern blot, diagnostic PCR and SQR activity assay. It is anticipated that the mitochondrial membrane potential was decreased in Pbsdha(-) parasites as a result of the knockout. Unexpectedly, the

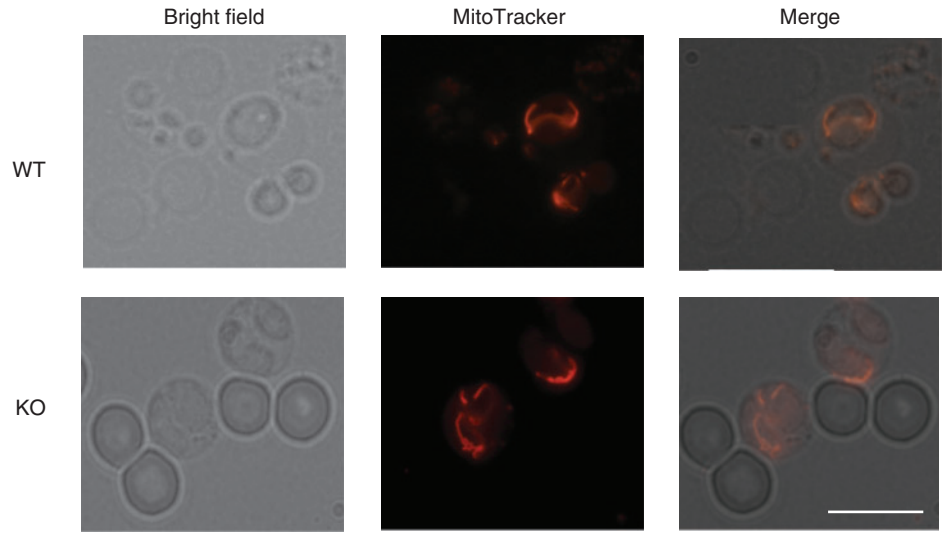

Fig. 5 MitoTracker staining of WT and Pbsdha(-) parasites. The erythrocytes infected with WT or Pbsdha(-) (KO) parasites was stained with MitoTracker to assess the integrity of the mitochondrial membrane potential. Bar represents 5 μm.

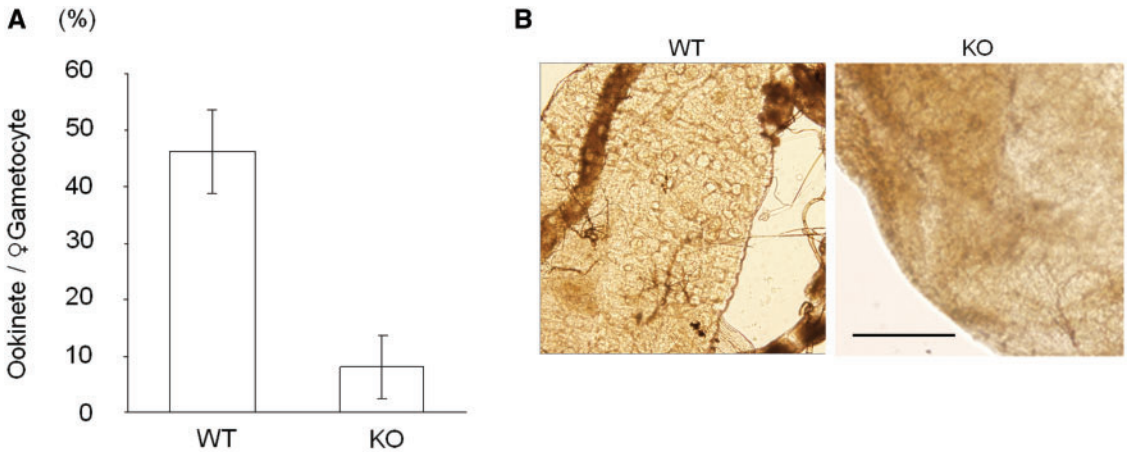

Fig. 6 Phenotypic analysis of Pbsdha(-) parasites. (A) Ookinete formation rate of WT and Pbsdha(-) (KO) parasites. The mouse blood infected with either WT or Pbsdha(-) parasites was incubated in fertilization medium to induce fertilization and differentiation into ookinetes. The ookinete formation rate was calculated by the percentage of female gametocytes, which converted into ookinetes. Error bars represents mean ± SD (n = 3). (B) Mosquito midguts infected with WT and Pbsdha(-) (KO) parasites. The latter carries no oocyst. Bars represent 200 μm.

Table III. Infectivity of WT and Pbsdha(-) parasites.

Parasite		Oocyst-positive mosquitoes	Mean oocysts/ midgut ± SD	Mouse infection
WT	Exp1	7/21	5.4 ± 11.3	+
	2	6/20	7.3 ± 6.4	+
	3	5/20	18.0 ± 30.3	+
	4	13/20	25.1 ± 30.5	+
	5	15/32	51.8 ± 63.4	+
Koa	Exp1	0/20	0	−
	2	0/20	0	−
	3	0/20	0	−
	4	0/20	0	−
	5	0/20	0	−
	6	0/20	0	−
Kob	Exp1	0/26	0	−

mitochondrial membrane potential seemed to be maintained in blood-stage parasites in the absence of complex II, which was demonstrated by the positive signal in MitoTracker staining. In addition to complex II, there are three other enzymes involved in electron flux that contribute to mitochondrial membrane potential; MQO (malate–quinone oxidoreductase), DHOD (dihydroorotate dehydrogenase) and NDH2 (type2 NADH–ubiquinone oxidoreductase), which is a single peptide dehydrogenase different from multi-subunit complex I (Fig. 7). It is therefore conceivable that any of these three enzymes may be a functional complement for the absence of complex II. Recently, it was reported that *P. berghei* lacking NDH2 (NDH2(-)) did keep mitochondrial membrane potential (*27*), supporting the hypothesis of mutual complementation among ETC enzymes.

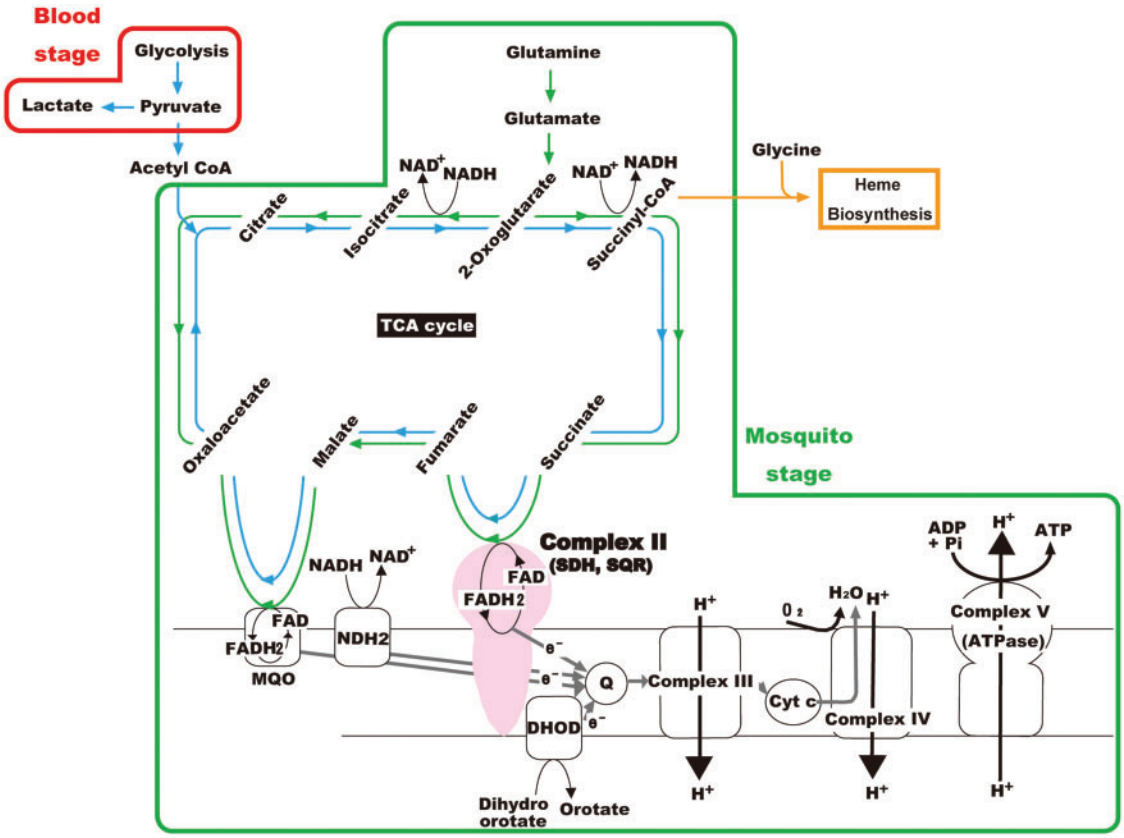

Fig. 7 Hypothetical Model of Plasmodial energy metabolism. Blue arrows represent canonical flow of glycolysis and TCA cycle. Green arrows represent *Plasmodium* TCA metabolism pathway. Unlike other eukaryotes, glycolysis (enclosed by red) does not link to TCA cycle. *Plasmodim* TCA cycle is initiated by uptaking of glutamine into mitochondria. Mitochondrial oxidative phosphorylation (enclosed by green) is essential for the parasite survival at mosquito stage because the Pbsdha(-) parasite is lethal at this stage.

Our phenotypic study revealed that Pbsdha(-) parasites proliferated and produced gametocytes with a similar rate to WT parasites in mice. Recently, we observed similar results in the blood-stage *P. falciparum*, of which Fp subunit was disrupted (Tanaka *et al.*, submitted for publication). *In vitro*, Pbsdha(-) male gametocytes differentiated to gametes (exflagellated) as WT ones, suggesting that complex II is not required for those developmental stages. It is known that mammalian sperm requires ATP for flagellum movement, which is supplied mainly from mitochondrial oxidative phosphorylation (*28*). While male gametes of malaria parasites show similar motility to that of mammalian sperm, it is obvious that parasite male gametes do not rely on oxidative phosphorylation because the male gametes do not possess mitochondria (*24*). This indicates that the driving force for male motility is exclusively supplied from glycolysis. The *in vitro* fertilization assay showed that Pbsdha(-) parasites were defect in ookinete formation. At this moment, it is not clear whether complex II is critical at female gametogenesis, fertilization or ookinete formation itself. Nevertheless, we speculate that the impact of *Pbsdha* gene disruption gave adverse influence on female, probably the stages after gametocytogenesis.

The most drastic phenotypic change in Pbsdha(-) parasites was the complete failure of oocyst formation. In malaria parasites, the ookinetes traverse midgut cell and arrive to the basal lamina where they transform into oocysts. In a single oocyst, mitosis occurs and several hundreds of sporozoites are generated inside. To accomplish such task, the parasites may need more ATP, which could be generated by oxidative phosphorylation. The complex II activity deletion may therefore adversely affect the oocyst formation. Recently, it was reported that NDH2(-) parasites developed normally in asexual stages but transformed into aberrant immature oocysts (*27*). Our present study together with this finding suggests that the ETC enzymes are essential in insect stages. However, there are several phenotypic differences between Pbsdha(-) and NDH2(-) parasites; 1) Pbsdha(-) parasites differentiated into ookinetes with low efficiency, while NDH2(-) ookinete formation is similar to WT parasites. This indicates that the Pbsdha deletion affects an earlier parasite stage compared with that of NDH2 deletion; 2) Pbsdha(-) parasites failed completely in oocyst formation, while NDH2(-) parasites formed immature oocysts with smaller size, demonstrating that the absence of complex II gives more severe defects in parasite development than NDH2 does. In other eukaryotes, it is known that mitochondrial complex II converts succinate to fumarate and reducing equivalents are transferred to quinone. In addition, complex II is one of the TCA cycle members

generating NADH, which is a substrate of NDH2. Thus, the deletion of complex II activity may render NDH2 unable to function in ETC. Severe phenotypic changes in Pbsdha(-) parasites could be therefore attributed to the aberration of NDH2 as well as complex II itself.

Conclusion

In the present work, we show that complex II has a critical role in insect-stage parasites. ETC is not only involved in ATP metabolism, but as well in heme biosynthesis (Fig. 7), which is also crucial for parasite survival (*29*). In addition to the ETC, complex II functions as the TCA cycle enzyme. Further studies are required to determine whether lack of any of these functions are the cause for the developmental arrest in Pbsdha(-) parasites. In any case, our study demonstrates that malaria parasite drastically switches energy metabolism when the parasites initiate sexual maturation and is subsequently introduced into the mosquito (Fig. 7).

The importance of complex II in insect-stage parasites suggests the possibility that complex II could be a novel target for transmission blocking (*30*). Previously, we reported that the amino acid sequences of the membrane anchor subunits CybL and CybS of *Plasmodium* complex II show exceptionally low homology to that of any other organism including human (*12*). In addition, our previous work revealed that atopenin A5 is a potent inhibitor against mammalian complex II with IC_{50} values of three-order of magnitudes lower than that of *Plasmodium* complex II (*13*). This indicates that 3D structure of ubiquinone-binding site in the parasitic complex II is quite distinct from those of mammalian complex II. Therefore, it is conceivable that the development of a parasitic complex II-specific inhibitor would be feasible by structure-based drug design targeting to the mosquito-stages parasite. Currently, further ATP metabolic gene knockout experiment using mouse malaria models are now in progress to draw general view of parasite energy metabolism in response to various environmental stimuli that may have been overlooked in *in vitro* culture systems as pointed out by Daily (*31*).

Acknowledgements

We thank Dr. Terenius for his comments on our manuscript.

Funding

Grants-in-aid for Creative Scientific Research (18GS0314 to KKand YW) and for Scientific Research (C) (21590467 to YY and 20590426 to MH) from the Japanese Society for the Promotion of Science, Targeted Proteins Research Program (to KK) and a Grant-in-aid for Scientific Research on Priority Areas (18073004 to KK and 210220044 to MH) and Grant-in-Aid for Scientific Research on Innovative Areas (22112519 to MH) from the Japanese Ministry of Education, Science, Culture, Sports and Technology, and a grant for research to promote the development of anti-AIDS pharmaceuticals from the Japan Health Sciences Foundation (to KK). This work was also partially suppored by Support Program for Scientific Research Platform in Private Universities (to HM) and SUMITOMO foundation (to MH).

Conflict of interest

None declared.

References

1. Snow, R.W., Guerra, C.A., Noor, A.M., Myint, H.Y., and Hay, S.I. (2005) The global distribution of clinical episodes of *Plasmodium falciparum* malaria. *Nature* **434**, 214–217
2. Petersen, I., Eastman, R., and Lanzer, M. (2011) Drug-resistant malaria: molecular mechanisms and implications for public health. *FEBS Lett.* **585**, 1551–1562
3. Foth, B.J., Stimmler, L.M., Handman, E., Crabb, B.S., Hodder, A.N., and McFadden, G.I. (2005) The malaria parasite *Plasmodium falciparum* has only one pyruvate dehydrogenase complex, which is located in the apicoplast. *Mol. Microbiol.* **55**, 39–53
4. Aikawa, M. (1966) The fine structure of the erythrocytic stages of three avian malarial parasites. *Plasmodium fallax, P. lophurae, and P. cathemerium. Am. J. Trop. Med. Hyg* **15**, 449–471
5. Bryant, C., Voller, A., and Smith, M.J. (1964) The incorporation of radioactivity from (14C)glucose into the soluble metabolic intermediates of malaria parasites. *Am. J. Trop. Med. Hyg* **13**, 515–519
6. Scheibel, L.W. and Pflaum, W.K. (1970) Cytochrome oxidase activity in platelet-free preparations of *Plasmodium falciparum*. *J. Parasitol.* **56**, 1054
7. Olszewski, K.L., Mather, M.W., Morrisey, J.M., Garcia, B.A., Vaidya, A.B., Rabinowitz, J.D., and Llinas, M. (2010) Branched tricarboxylic acid metabolism in *Plasmodium falciparum*. *Nature* **466**, 774–778
8. Hall, N., Karras, M., Raine, J.D., Carlton, J.M., Kooij, T.W., Berriman, M., Florens, L., Janssen, C.S., Pain, A., Christophides, G.K., James, K., Rutherford, K., Harris, B., Harris, D., Churcher, C., Quail, M.A., Ormond, D., Doggett, J., Trueman, H.E., Mendoza, J., Bidwell, S.L., Rajandream, M.A., Carucci, D.J., Yates, J.R. 3rd, Kafatos, F.C., Janse, C.J., Barrell, B., Turner, C.M., Waters, A.P., and Sinden, R.E. (2005) A comprehensive survey of the *Plasmodium* life cycle by genomic, transcriptomic, and proteomic analyses. *Science* **307**, 82–86
9. Krungkrai, J., Prapunwattana, P., and Krungkrai, S.R. (2000) Ultrastructure and function of mitochondria in gametocytic stage of *Plasmodium falciparum*. *Parasite* **7**, 19–26
10. Maklashina, E. and Cecchini, G. (2010) The quinone-binding and catalytic site of complex II. *Biochim. Biophys. Acta.* **1797**, 1877–1882
11. Takeo, S., Kokaze, A., Ng, C.S., Mizuchi, D., Watanabe, J.I., Tanabe, K., Kojima, S., and Kita, K. (2000) Succinate dehydrogenase in *Plasmodium falciparum* mitochondria: molecular characterization of the SDHA and SDHB genes for the catalytic subunits, the flavoprotein (Fp) and iron-sulfur (Ip) subunits. *Mol. Biochem. Parasitol.* **107**, 191–205
12. Mogi, T. and Kita, K. (2009) Identification of mitochondrial Complex II subunits SDH3 and SDH4 and ATP synthase subunits a and b in Plasmodium spp. *Mitochondrion* **9**, 443–453
13. Kawahara, K., Mogi, T., Tanaka, T.Q., Hata, M., Miyoshi, H., and Kita, K. (2009) Mitochondrial dehydrogenases in the aerobic respiratory chain of the rodent malaria parasite *Plasmodium yoelii yoelii*. *J. Biochem.* **145**, 229–237
14. Takashima, E., Takamiya, S., Takeo, S., Mi-ichi, F., Amino, H., and Kita, K. (2001) Isolation of

mitochondria from *Plasmodium falciparum* showing dihydroorotate dependent respiration. *Parasitol. Int.* **50**, 273–278

15. Mather, M.W., Morrisey, J.M., and Vaidya, A.B. (2010) Hemozoin-free *Plasmodium falciparum* mitochondria for physiological and drug susceptibility studies. *Mol. Biochem. Parasitol.* **174**, 150–153
16. Hirai, M., Wang, J., Yoshida, S., Ishii, A., and Matsuoka, H. (2001) Characterization and identification of exflagellation-inducing factor in the salivary gland of *Anopheles stephensi* (Diptera: Culicidae). *Biochem. Biophys. Res. Commun.* **287**, 859–864
17. Dessens, J.T., Beetsma, A.L., Dimopoulos, G., Wengelnik, K., Crisanti, A., Kafatos, F.C., and Sinden, R.E. (1999) CTRP is essential for mosquito infection by malaria ookinetes. *EMBO J.* **18**, 6221–6227
18. Janse, C.J., Ramesar, J., and Waters, A.P. (2006) High-efficiency transfection and drug selection of genetically transformed blood stages of the rodent malaria parasite *Plasmodium berghei*. *Nat. Protoc.* **1**, 346–356
19. Jensen, J.B. and Trager, W. (1977) *Plasmodium falciparum* in culture: use of outdated erthrocytes and description of the candle jar method. *J. Parasitol.* **63**, 883–886
20. Kobayashi, T., Sato, S., Takamiya, S., Komaki-Yasuda, K., Yano, K., Hirata, A., Onitsuka, I., Hata, M., Miichi, F., Tanaka, T., Hase, T., Miyajima, A., Kawazu, S., Watanabe, Y., and Kita, K. (2007) Mitochondria and apicoplast of *Plasmodium falciparum*: behaviour on subcellular fractionation and the implication. *Mitochondrion* **7**, 125–132
21. Chan, M., Tan, D.S., Wong, S.H., and Sim, T.S. (2006) A relevant in vitro eukaryotic live-cell system for the evaluation of plasmodial protein localization. *Biochimie* **88**, 1367–1375
22. van Dijk, M.R., Janse, C.J., Thompson, J., Waters, A.P., Braks, J.A., Dodemont, H.J., Stunnenberg, H.G., van Gemert, G.J., Sauerwein, R.W., and Eling, W. (2001) A central role for P48/45 in malaria parasite male gamete fertility. *Cell* **104**, 153–164
23. Okamoto, N., Spurck, T.P., Goodman, C.D., and McFadden, G.I. (2009) Apicoplast and mitochondrion in gametocytogenesis of *Plasmodium falciparum*. *Eukaryot. Cell* **8**, 128–132
24. Mogi, T. and Kita, K. (2010) Diversity in mitochondrial metabolic pathways in parasitic protists *Plasmodium* and *Cryptosporidium*. *Parasitol. Int.* **59**, 305–312
25. van Dooren, G.G., Marti, M., Tonkin, C.J., Stimmler, L.M., Cowman, A.F., and McFadden, G.I. (2005) Development of the endoplasmic reticulum, mitochondrion and apicoplast during the asexual life cycle of *Plasmodium falciparum*. *Mol. Microbiol.* **57**, 405–419
26. Daily, J.P., Scanfeld, D., Pochet, N., Le Roch, K., Plouffe, D., Kamal, M., Sarr, O., Mboup, S., Ndir, O., Wypij, D., Levasseur, K., Thomas, E., Tamayo, P., Dong, C., Zhou, Y., Lander, E.S., Ndiaye, D., Wirth, D., Winzeler, E.A., Mesirov, J.P., and Regev, A. (2007) Distinct physiological states of *Plasmodium falciparum* in malaria-infected patients. *Nature* **450**, 1091–1095
27. Boysen, K.E. and Matuschewski, K. (2011) Arrested oocyst maturation in *Plasmodium* parasites lacking type II NADH:ubiquinone dehydrogenase. *J. Biol. Chem.* **286**, 32661–3271
28. Nascimento, J.M., Shi, L.Z., Tam, J., Chandsawangbhuwana, C., Durrant, B., Botvinick, E.L., and Berns, M.W. (2008) Comparison of glycolysis and oxidative phosphorylation as energy sources for mammalian sperm motility, using the combination of fluorescence imaging, laser tweezers, and real-time automated tracking and trapping. *J. Cell Physiol.* **217**, 745–751
29. Nagaraj, V.A., Arumugam, R., Prasad, D., Rangarajan, P.N., and Padmanaban, G. (2010) Protoporphyrinogen IX oxidase from *Plasmodium falciparum* is anaerobic and is localized to the mitochondrion. *Mol. Biochem. Parasitol.* **174**, 44–52
30. Lavazec, C. and Bourgouin, C. (2008) Mosquito-based transmission blocking vaccines for interrupting *Plasmodium* development. *Microbes Infect.* **10**, 845–849
31. LeRoux, M., Lakshmanan, V., and Daily, J.P. (2009) *Plasmodium falciparum* biology: analysis of in vitro versus in vivo growth conditions. *Trends Parasitol.* **25**, 474–481